

# Development of an Extended Operational States Observer of a Power Assist Wheelchair

Sehoon Oh

Institute of Industrial Science  
University of Tokyo  
4-6-1, Komaba, Meguro, Tokyo, 153-8505 Japan  
sehoon@horilab.iis.u-tokyo.ac.jp  
http://mizugaki.iis.u-tokyo.ac.jp/

Yoichi Hori

Institute of Industrial Science  
University of Tokyo  
4-6-1, Komaba, Meguro, Tokyo, 153-8505 Japan  
hori@iis.u-tokyo.ac.jp  
http://mizugaki.iis.u-tokyo.ac.jp/

*Abstract*— An operational state observer for a wheelchair system we have proposed is extended to three dimensions. This new observer incorporates a 3-axis accelerometer allowing the user to estimate more precise information on conditions of hills for the lateral direction.

First, a model dynamics illustrating the relationship between the gravity in the lateral direction and the motion of a wheelchair on a slope is derived. Experimental results verify our derivation of equations. Then, the dynamics is simplified and used in the design of the extended observer. Since the dynamics itself and the output of that have nonlinear characteristics, the extended kalman filter design algorithm is employed. By simulation, the stability and effectiveness of the application is verified.

*Key Words* : wheelchair, operational states observer, extended kalman filter, 2-dimensional effect of the gravity, human friendly motion control

## I. INTRODUCTION

We have suggested an operational state observer that provides important operational conditions in [1]. This paper improves the observer into 3 dimensions.

### A. Operational State Observer in a Power-assisted Wheelchair

In [1], operational states described in Figure 1 (a) are accurately estimated using the kalman filter algorithm. Figure 1 (b) is the measurements this observer uses.

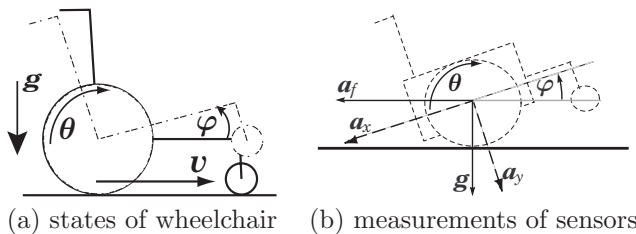


Fig. 1. Operational States and Measured Information

Since it employs a two-dimensional accelerometer, any information on the lateral direction is not measurable. The gravity acting in the lateral direction, illustrated in Figure 2 will not be estimated in this observer although it interferes with the heading direction of a wheelchair.

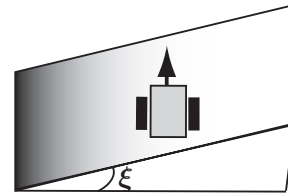


Fig. 2. Gravity acting laterally on a wheelchair

### B. Extension of Conventional Operational State Observer

If the angle  $\xi$  of the slope is obtainable, it must improve the control of a wheelchair. For this reason, we design a novel states observer to get information of the angle  $\xi$ .

Figure 3 illustrates the angles we will estimate by a novel observer design: the pitch angle of a wheelchair ( $\varphi$ ) with regarding to its heading direction, the heading angle ( $\alpha$ ) with regard to the horizon and the slope angle ( $\xi$ ) of a hill.

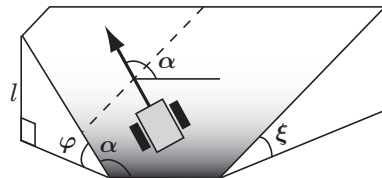


Fig. 3. Angles Necessary for Safe Operation on a Slope

If we can distinguish these angles correctly from the measured values, the control of a wheelchair on a slope will be more safe and easy to operate by a user. For example, accurate values of these angles enable a controller to drive a wheelchair straightly in the face of the lateral gravity.

## II. DESCRIPTION OF THREE-DIMENSIONAL OPERATIONAL STATE

In order to design a states observer, the relationship of operational states, especially the angles to be estimated should be analyzed at first.

### A. Derivation of Output Equations Produced by Three Sensors

Three kinds of sensors are utilized in this system: one 3-axis accelerometer, two encoders on both wheels and one

gyroscope which measures the pitch angle around the axis of wheels. These sensors provide  $\varphi$ ,  $\alpha$ ,  $\xi$  in Figure 3 and the moving velocity  $v$  in Figure 1 (a).

In order to design an observer using these sensor outputs, the relationship between these outputs and state variables should be clarified. At first, output equations which tell how the state variables appear in sensor outputs are derived here.

Figure 3 shows the relationship between the pitch angle  $\varphi$  and the yaw or heading angle  $\alpha$  of a wheelchair on a slope of  $\xi$ . This relationship will be described as Equation (1).

$$\sin \varphi = \sin \alpha \sin \xi \quad (1)$$

This equation reveals the output equation of the gyroscope which measures the angular velocity of  $\varphi$ . The equation is given as Equation (3).

$$\dot{\varphi} = \sin^{-1}(\sin \alpha \sin \xi) \simeq \sin \alpha \sin \xi \quad (2)$$

$$\dot{\varphi} \simeq \dot{\alpha} \cos \alpha \sin \xi + \dot{\xi} \sin \alpha \cos \xi \quad (3)$$

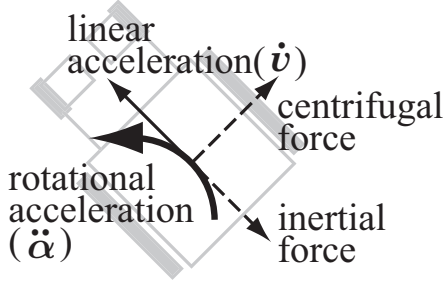


Fig. 4. Decomposition of the force measured by an accelerometer

Accelerometer measures the linear acceleration of the wheelchair including the gravity vector. In addition to the heading acceleration in the linear direction, yaw acceleration is also measured by a 3-axis acceleration. Equation (4) to (6) describe the output equations of a 3-axis accelerometer.

$$a_x = g \sin \xi \sin \alpha + \dot{v} + f_{\text{rotation}_x} \quad (4)$$

$$a_y = g \sin \xi \cos \alpha + v \dot{\alpha} + f_{\text{rotation}_y} \quad (5)$$

$$a_z = g \cos \xi, \quad (6)$$

where  $v$  illustrates the velocity of a wheelchair in its heading angle. The directions of  $x, y, z$  axes are illustrated in Figure 5.

The first term of each equation shows the gravity vector of which direction is determined by the condition  $\alpha, \xi$  of a hill the wheelchair is located. The second terms represent the inertial force in Equation (4) and the centrifugal force in Equation (5). These are the forces manifested on the center of mass.

Meanwhile,  $f_{\text{rotation}_{x,y}}$  are the forces caused by the fact that the accelerometer is not located in the center of mass of the wheelchair. Rotational motion around the center of mass produces additional acceleration measurements in the accelerometer. Figure 5 (a) shows the location of the

accelerometer in a wheelchair. Since it is  $\Delta_x, \Delta_y$  off the center, additional inertial and centrifugal forces are applied to the accelerometer described in Equation (7) and (8).

$$f_{\text{rotation}_x} = \ddot{\alpha} \Delta_x + m \dot{\alpha}^2 \Delta_y \quad (7)$$

$$f_{\text{rotation}_y} = -\ddot{\alpha} \Delta_y + m \dot{\alpha}^2 \Delta_x \quad (8)$$

First terms are the output of the inertial force and second terms are the output of the centrifugal force. Notice that  $\Delta_y$  would be 0 if  $v$  is calculated as the linear velocity at the location of the accelerometer.

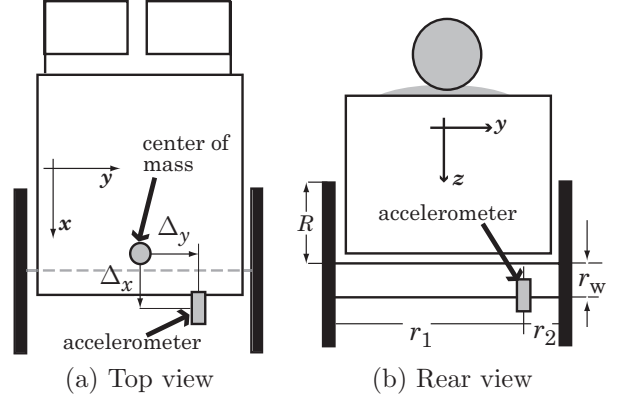


Fig. 5. Location of an Accelerometer in a Wheelchair

If the slip between the wheels and the ground is ignored, the rotated angles of two wheels which are represented as  $\theta_l, \theta_r$  here, can be associated with the measured acceleration.  $v$  at the location of the accelerometer is identified with Equation (9) using  $\theta_l, \theta_r$ .

$$v = \frac{r_2}{r_1 + r_2} R \dot{\theta}_r + \frac{r_1}{r_1 + r_2} R \dot{\theta}_l, \quad (9)$$

where  $r_1, r_2, R$  means the lengths and distances illustrated in Figure 5. Also the heading angle  $\alpha$  in Equation (5) can be derived from  $\theta_l$  and  $\theta_r$  as Equation (10) assuming no slip.

$$\alpha = \frac{R}{r_1 + r_2} (\theta_r - \theta_l) \quad (10)$$

Finally we obtain 6 output equations of all sensors, which contain the values of  $\varphi, \alpha, \xi$  we want to estimate. The equations are re-described in Table I.

TABLE I  
OUTPUT EQUATIONS

Gyroscope	$\dot{\varphi} = \dot{\alpha} \cos \alpha \sin \xi + \dot{\xi} \sin \alpha \cos \xi$
Accelerometer	$a_x = g \sin \xi \sin \alpha + \dot{v} + m \dot{\alpha}^2 \Delta_y$
	$a_y = g \sin \xi \cos \alpha + v \dot{\alpha} - \ddot{\alpha} \Delta_y$
	$a_z = g \cos \xi$
Encoder	$v = \frac{r_2}{r_1 + r_2} R \dot{\theta}_r + \frac{r_1}{r_1 + r_2} R \dot{\theta}_l$
	$\alpha = \frac{R}{r_1 + r_2} (\theta_r - \theta_l)$

While the equation of  $a_x$  is straightforward, the equation of  $a_y$  is somewhat complicated. In order to verify

that equation, three kinds of experiments are performed: 1) wheelchair rotates its heading angle without moving forward, 2) it turns right, 3) it goes forward and moves backward turning left.

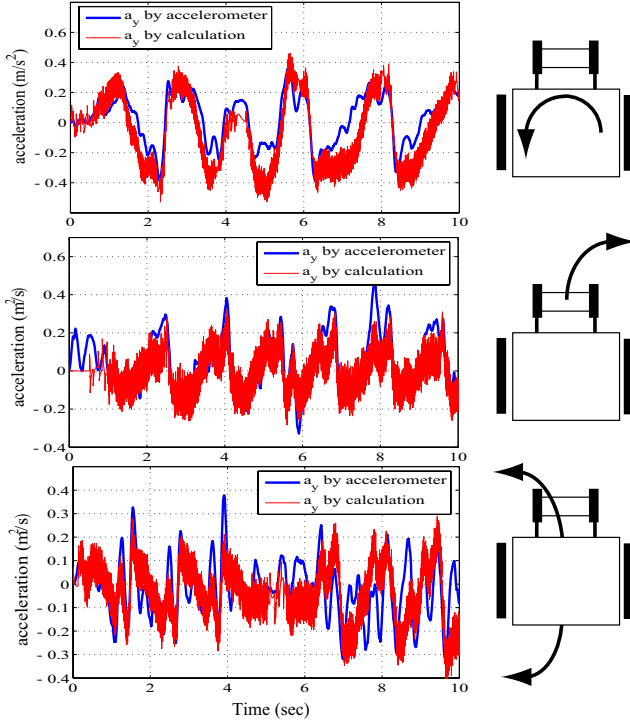


Fig. 6. Comparison of Lateral Acceleration

In Figure 6,  $a_y$  described as a thick blue line represents the lateral acceleration measured by the accelerometer, while the thick blue line represents  $a_y$  calculated based on Equation (5) with the value of  $v$  and  $\alpha$  from the encoder output. Two values are identified with each other, proving the correctness of Equation (5).

### B. Derivation of Three-dimensional Dynamics

In order to build an state observer, a model of wheelchair dynamics is required. For this reason, more precise modeling of dynamics is necessary to describe how external force or the gravity affects on the motion of a wheelchair in the lateral direction. Since the lateral disturbance affects on the lateral motion of the wheelchair through the tires, the model should include the cornering force of the tires. This point is quite similar with the analysis on the dynamics of four-wheel vehicle. For this similarity, the modeling of vehicle dynamics is adopted to explain the lateral motion of a wheelchair.

Figure 7 shows the relationship between the direction of moving velocity and heading direction. The difference is called as  $\beta$  or the slip angle in the vehicle engineering. When the gravity acts on the wheelchair in the lateral direction, that lateral force brings about the slip angle causing tire to produce cornering force. Finally the gravity results in the change of the heading angle. This relationship between the dynamics of  $\beta$  and the yaw rate  $\gamma$  is described

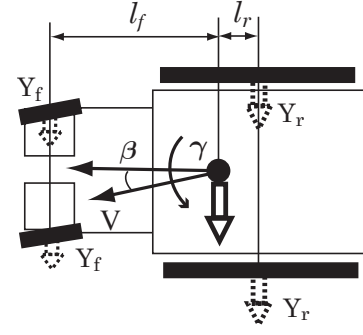


Fig. 7. Lateral Motion of a Wheelchair

in Equation (11) and (12).

$$mV \left( \frac{d\beta}{dt} + \gamma \right) = Y_f(\beta_f, \gamma) + Y_r(\beta_r, \gamma) + g_{lat} \quad (11)$$

$$I \frac{d\gamma}{dt} = l_f Y_f(\beta_f, \gamma) - l_r Y_r(\beta_r, \gamma), \quad (12)$$

where  $Y_f, Y_r$  mean the cornering force acting on the front wheels and the rear wheels (Figure 7).

This theory is well-known in the researches of vehicles. The most different point of a wheelchair dynamics from that of a four-wheel vehicle is that the front wheels consist of casters and are not fixed so that the heading angle of the front wheels can be identified with the direction of the wheelchair's moving velocity,  $V$  in Figure 7. This means  $\beta_s$  in the front wheels is quite small and there will be little cornering force in the front wheels. Based on this assumption, the cornering forces  $Y_f, Y_r$  are given as the following.

$$Y_f = -K_f \beta_f = 0 \quad (13)$$

$$Y_r = -K_r \beta_r = -K_r \left( \beta - l_r \frac{\gamma}{V} \right) \quad (14)$$

Based on these consideration, the transfer function from the gravity to the rotated angle  $\alpha = \int \gamma dt$  which we want to estimate, is given as a second order system. However, we try to approximate it to a first order time delay system.

$$\frac{\gamma}{g_{lat}} = \frac{\dot{\alpha}}{g_{lat}} = \frac{K}{s^2 + 2\zeta\omega_n s + \omega_n^2} \rightarrow \frac{K}{s + \omega_o} \quad (15)$$

In this approximation, the error in the phase is the biggest problem. However, the gravity does not changes

$$\dot{x}_l = -\frac{D}{M} \dot{x}_l + \frac{1}{M} (u_f - M g \sin \alpha \sin \xi) \quad (16)$$

$$\ddot{\alpha} = -\frac{B}{I} \dot{\alpha} + \frac{1}{I} (u_r - M g l_r \cos \alpha \sin \xi) \quad (17)$$

$\dot{x}_5$  should be considered as a state since it is measured in the gyroscope.

$$\begin{aligned} \mathbf{x} &= (x_l \quad \alpha \quad \dot{x}_l \quad \dot{\alpha} \quad \xi \quad \dot{\xi})^T \\ &= (x_1 \quad x_2 \quad x_3 \quad x_4 \quad x_5 \quad x_6)^T \end{aligned} \quad (18)$$

$$\begin{aligned}\dot{\mathbf{x}} &= \begin{pmatrix} x_3 \\ x_4 \\ -\frac{D}{M}x_3 - g \sin x_2 \sin x_5 \\ -\frac{E}{T}x_4 - \frac{M}{T}g \cos x_2 \sin x_5 \\ x_6 \\ 0 \end{pmatrix} + \begin{pmatrix} 0 \\ 0 \\ \frac{1}{M}u_f \\ \frac{1}{T}u_\tau \\ 0 \\ 0 \end{pmatrix} \\ &= \mathbf{f}(\mathbf{x}) + \mathbf{g}(\mathbf{u})\end{aligned}\quad (19)$$

$$\begin{aligned}\mathbf{y} &= \begin{pmatrix} x_1 \\ x_2 \\ x_4 \cos x_2 \sin x_5 + x_6 \sin x_2 \cos x_5 \\ \dot{x}_3 + g \sin x_2 \sin x_5 + m_{acc}d_{accx}x_4^2 \\ Mx_3x_4 + g \cos x_2 \sin x_5 + m_{acc}d_{accy}x_4^2 \\ g \cos x_5 \end{pmatrix} \\ &= \begin{pmatrix} x_1 \\ x_2 \\ x_4 \cos x_2 \sin x_5 + x_6 \sin x_2 \cos x_5 \\ -\frac{D}{M}x_3 + m_{acc}d_{accx}x_4^2 + \frac{1}{M}u_f \\ Mx_3x_4 + g \cos x_2 \sin x_5 + m_{acc}d_{accy}x_4^2 \\ g \cos x_5 \end{pmatrix} \\ &= \mathbf{h}(\mathbf{x}, \mathbf{u})\end{aligned}\quad (20)$$

Notice that we include  $\xi$  and  $\dot{\xi}$  as a state. Changes in  $\xi$  or the slope angle are random and difficult to model. If we include this change as a disturbance state, it will simplify the model. This idea will be verified in simulations in Section IV.

### III. DESIGN OF NONLINEAR OPERATIONAL STATE OBSERVER FOR A WHEELCHAIR

With the equations derived in last section, an operational state observer is designed in this section.

#### A. Basic Design of Kalman Filter

Kalman filter design is adopted for the design of the state observer due to the characteristics of the motion and output equations: at first, it has multi-output so that it is not easy to decide the observer gain using pole assignment. Secondly, the dynamics has nonlinear characteristic. Kalman filter design can deal with these characteristics.

If a system is a linear system, it can be modeled as

$$\mathbf{x}(t) = \mathbf{A}\mathbf{x}(t-1) + \mathbf{B}\mathbf{u}(t-1) + \mathbf{v}(t), \quad (21)$$

$$\mathbf{y}(t) = \mathbf{C}\mathbf{x}(t) + \mathbf{e}(t), \quad (22)$$

where  $\mathbf{v}(t)$  and  $\mathbf{e}(t)$  are white noise sequences with zero mean and covariance matrix

$$\mathbf{E} \begin{pmatrix} \mathbf{v}(t) \\ \mathbf{e}(t) \end{pmatrix} \begin{pmatrix} \mathbf{v}^T(t) & \mathbf{e}^T(t) \end{pmatrix} = \begin{pmatrix} \mathbf{V} & \mathbf{0} \\ \mathbf{0} & \mathbf{R} \end{pmatrix}. \quad (23)$$

Design of Kalman filter is formulated only for linear systems so that the following explanation considers the above linear system as the target system. However, this design is also applicable to the nonlinear systems and it will be

addressed later. The design has two procedures: the prediction based on a model dynamics and the update driven by the output innovation  $(\mathbf{y}(t) - \hat{\mathbf{y}}(t))$

$$\bar{\mathbf{x}}(t) = \mathbf{A}\mathbf{x}(t-1) + \mathbf{B}\mathbf{u}(t-1) \quad (24)$$

$$\hat{\mathbf{y}}(t) = \mathbf{C}\bar{\mathbf{x}}(t) \quad (25)$$

$$\hat{\mathbf{x}}(t) = \bar{\mathbf{x}}(t) + \mathbf{K}(\mathbf{y}(t) - \hat{\mathbf{y}}(t)). \quad (26)$$

Equation (24) describes the prediction procedure, and Equation (26) describes the update procedure. The observer gain  $\mathbf{K}(t)$  is mainly related with the stability of the observer. Kalman filter determines the  $\mathbf{K}$  to minimize the prediction error covariance when given system noise and measurement noise.

Kalman filter focuses on the transition of the covariance of estimation error  $\mathbf{P}(t-1|t-1) = \mathbf{E}((\mathbf{x}(t-1) - \hat{\mathbf{x}}(t-1))(\mathbf{x}(t-1) - \hat{\mathbf{x}}(t-1))^T)$ . By the prediction procedure this covariance will be changed as

$$\mathbf{P}(t|t-1) = \mathbf{A}\mathbf{P}(t-1|t-1)\mathbf{A}^T + \mathbf{V}. \quad (27)$$

$\mathbf{V}$  is the covariance given in Equation (23). This covariance is accumulated through the update procedure. In addition to this change,  $\mathbf{R}_{yy}$  and  $\mathbf{R}_{xy}$  are also necessary to calculate the estimation error covariance matrix.

$$\mathbf{R}_{yy}(t) = \mathbf{C}\mathbf{P}(t|t-1)\mathbf{C}^T + \mathbf{R} \quad (28)$$

$$\mathbf{R}_{xy} = \mathbf{P}(t|t-1)\mathbf{C}^T \quad (29)$$

With these matrixes, the error covariance will be updated as

$$\begin{aligned}\mathbf{P}(t|t) &= \mathbf{E}((\mathbf{x}(t) - \hat{\mathbf{x}}(t))(\mathbf{x}(t) - \hat{\mathbf{x}}(t))^T) \\ &= \mathbf{E}((\mathbf{x}(t) - \bar{\mathbf{x}}(t) - \mathbf{K}(t)\tilde{\mathbf{y}}(t))(\mathbf{x}(t) - \bar{\mathbf{x}}(t) - \mathbf{K}(t)\tilde{\mathbf{y}}(t))^T) \\ &= \mathbf{P}(t|t-1) - \mathbf{K}(t)\mathbf{R}_{xy}^T - \mathbf{R}_{xy}\mathbf{K}^T(t) + \mathbf{K}(t)\mathbf{R}_{yy}\mathbf{K}(t).\end{aligned}\quad (30)$$

This transition of covariance matrix makes clear what  $\mathbf{K}$  will optimize the covariance. In order to minimize Equation (30),  $\mathbf{K}(t)$  should be give as

$$\mathbf{K}(t) = \mathbf{R}_{xy}\mathbf{R}_{yy}^{-1}. \quad (31)$$

Then corrected covariance will be

$$\mathbf{P}(t|t) = \mathbf{P}(t|t-1) - \mathbf{R}_{xy}\mathbf{R}_{yy}^{-1}\mathbf{R}_{xy}^T. \quad (32)$$

#### B. Extension of Kalman Filter to Nonlinear Region

Although the design in the last section is for the linear systems, it is also applicable to nonlinear system. The extended kalman filter (EKF) computes the gain  $\mathbf{K}(t)$  by linearizing nonlinear system. Let us consider a nonlinear model

$$\mathbf{x}(t) = \mathbf{f}(\mathbf{x}(t-1)) + \mathbf{g}(\mathbf{u}(t-1), \mathbf{x}) + \mathbf{v}(t), \quad (33)$$

$$\mathbf{y}(t) = \mathbf{h}(\mathbf{x}(t)) + \mathbf{e}(t), \quad (34)$$

where  $\mathbf{v}(t)$  and  $\mathbf{e}(t)$  are white noise sequences with zero mean and covariance matrix (Eq. (23)).

Based on these model equations, the two procedures of Kalman filter, the prediction and the update would be given as

$$\bar{\mathbf{x}}(t) = \mathbf{f}(\mathbf{x}(t-1)) + \mathbf{g}(\mathbf{u}(t-1)) \quad (35)$$

$$\hat{\mathbf{y}}(t) = \mathbf{h}(\bar{\mathbf{x}}(t)) \quad (36)$$

$$\hat{\mathbf{x}}(t) = \bar{\mathbf{x}}(t) + \mathbf{K}(t)(\mathbf{y}(t) - \hat{\mathbf{y}}(t)) \quad (37)$$

The problem is the decision of the gain  $\mathbf{K}(t)$  which will optimize the covariance of estimation error under a certain system and measurement noises. Noting that the optimization in linear systems is done calculating the transition of error covariance matrix, we can understand that the same optimization can be conducted if we can calculate the transition equation in nonlinear systems. From this viewpoint, linearization approximation becomes necessary.

If we adopt the Taylor expansion for linearization, three matrixes in Equation (38) to (40) will linearize the nonlinear system.

$$\mathbf{F}(t) = \left. \frac{\partial \mathbf{f}(t, \mathbf{x})}{\partial \mathbf{x}} \right|_{\mathbf{x}=\hat{\mathbf{x}}(t)} \quad (38)$$

$$\mathbf{G}(t) = \mathbf{g}(\mathbf{x})|_{\mathbf{x}=\hat{\mathbf{x}}(t)} \quad (39)$$

$$\mathbf{H}(t) = \left. \frac{\partial \mathbf{h}(t, \mathbf{x})}{\partial \mathbf{x}} \right|_{\mathbf{x}=\hat{\mathbf{x}}(t)} \quad (40)$$

With these matrixes, the estimation error covariance matrix  $\mathbf{P}(t+1|t)$  and the gain  $\mathbf{K}(t)$  will be given as

$$\mathbf{K}(t) = \mathbf{P}(t|t-1)\mathbf{H}^T(t)(\mathbf{H}(t)\mathbf{P}(t|t-1)\mathbf{H}^T(t) + \mathbf{R})^{-1} \quad (41)$$

$$\mathbf{P}(t|t) = \mathbf{P}(t|t-1) - \mathbf{K}(t)\mathbf{H}(t)\mathbf{P}(t|t-1) \quad (42)$$

$$\mathbf{P}(t+1|t) = \mathbf{F}(t)\mathbf{P}(t|t)\mathbf{F}^T(t) + \mathbf{G}(t)\mathbf{V}(t)\mathbf{G}^T(t), \quad (43)$$

where  $\mathbf{R}$  and  $\mathbf{V}$  are the covariance matrixes in Equation (23). We can see these equations are very similar with the equations (27) to (32) in linear systems.

We should notice that since the gain  $\mathbf{K}(t)$  is derived from the approximation, it is likely to estimate the states correctly but is not an optimal one. To overcome this incorrectness, other observer designs such as the unscented filter [3] are proposed.

### C. Application of Extended Kalman Filter to a Wheelchair

In order to apply this EKF design to our observer, three matrixes  $\mathbf{F}(t)$ ,  $\mathbf{G}(t)$  and  $\mathbf{H}(t)$  should be derived from the equation (19) and (20). Equation (44) and (45) represents the derived linearizing matrixes.

With these matrixes, an extended operational state observer for a wheelchair is designed. In the next section, we will verify our design using simulations.

## IV. SIMULATION RESULTS

Main purposes of simulations conducted in this section are two: one is the verification of observer design, which means it will be checked whether the extended operational state observer can correctly estimate the states in spite of the linearization approximation done in EKF design. The

other is the verification of how effect it is to introduce  $\xi$  and  $\hat{\xi}$  as states.

Three cases are simulated: 1) a wheelchair goes up a hill perpendicular to the horizon, 2) a wheelchair goes up a hill not perpendicular to the horizon, 3) a wheelchair attempts to change its heading angle on a hill.

At first, when a wheelchair climbs a hill perpendicular to the horizon, the gravity affects only the moving velocity and the state  $\alpha$  will keep its value as  $\frac{\pi}{2}$ . Figure 8 shows the

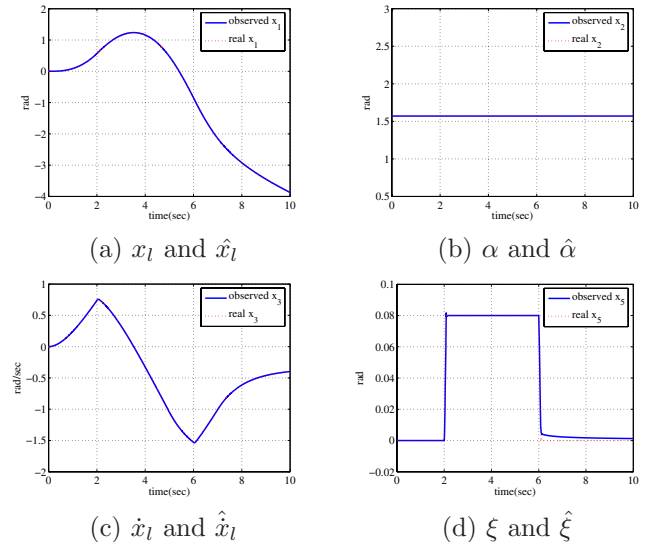


Fig. 8. Simulation 1) Perpendicular Climbing

result of this perpendicular climbing simulation. Changes in  $\xi$  means a wheelchair goes up a hill of 0.08 rad from 2 to 6 second. Since torque to propel a wheelchair in the longitudinal direction is applied to a wheelchair (the pattern of torque is illustrated in Figure 9 (f)), it starts to move and the state  $x_l$  increases for the moment. However, after the wheelchair goes up a hill  $x_l$  and  $\dot{x}_l$  start to decrease. This is simulated in the result, and we can check that the proposed observer correctly estimates the states.

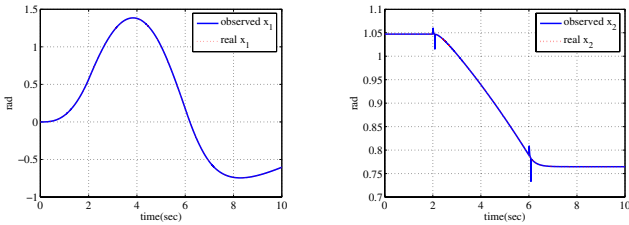
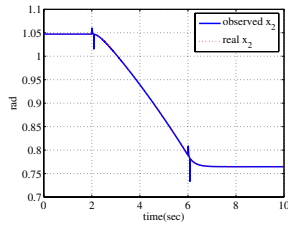
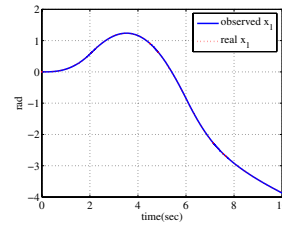
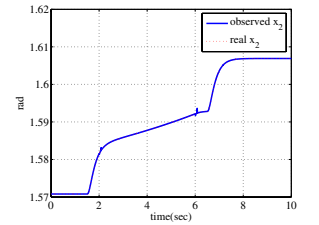
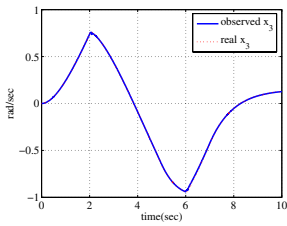
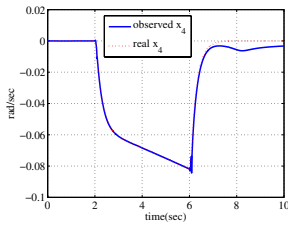
Figure 9 is the simulation result when a wheelchair goes up a hill with  $\alpha = \frac{\pi}{3}$ . If the heading angle is not perpendicular to the horizon, the gravity affects the heading angle and makes the wheelchair turn. This motions is well simulated and we can see in Figure (b) that  $\alpha$  moves to  $-\frac{\pi}{2}$  due to the gravity. The proposed observer can correctly estimate the states also in this case. However,  $\hat{\xi}$ , the observed slope angle is somewhat incorrect. Since the state  $\xi$  does not have any model and is only handled as a disturbance, these incorrectness cannot be avoided.

Figure 10 is the simulation results of a wheelchair on which a user attempts to change the heading angle at 1.5 and 6.5 seconds. Figure (f) shows the yaw moment applied by a user.

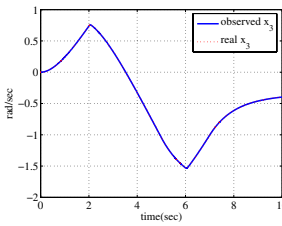
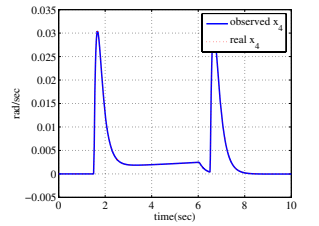
Around 1.5 second,  $\alpha$  starts to increase from  $\frac{\pi}{2}$  by the yaw moment. After 2 second, the gravity starts to affect  $\alpha$  since it is not perpendicular to the horizon.  $\alpha$  increases due to the gravity from 2 to 6 second. After 6 second, the wheelchair is on level ground again and  $\alpha$  is only driven by the applied yaw moment.

$$F(t) = \begin{pmatrix} 0 & 0 & 1 & 0 & 0 & 0 \\ 0 & 0 & 0 & 1 & 0 & 0 \\ 0 & -g \cos x_2 \sin x_5 & -\frac{D}{M} & 0 & -g \sin x_2 \cos x_5 & 0 \\ 0 & \frac{M}{I} g \sin x_2 \sin x_5 & 0 & -\frac{B}{I} & -\frac{M}{I} g \cos x_2 \cos x_5 & 0 \\ 0 & 0 & 0 & 0 & 0 & 1 \\ 0 & 0 & 0 & 0 & 0 & 0 \end{pmatrix} \quad (44)$$

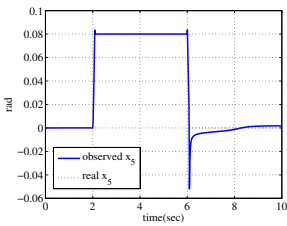
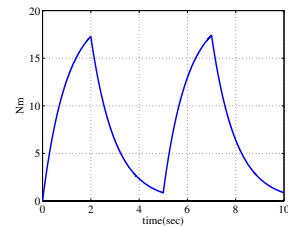
$$H(t) = \begin{pmatrix} 1 & 0 & 0 & 0 & 0 & 0 \\ 0 & 1 & 0 & 0 & 0 & 0 \\ 0 & -x_4 \sin x_2 \sin x_5 + x_6 \cos x_2 \cos x_5 & 0 & \cos x_2 \sin x_5 & x_4 \cos x_2 \cos x_5 - x_6 \sin x_2 \sin x_5 & \sin x_2 \cos x_5 \\ 0 & 0 & -\frac{D}{M} & 2m_{acc}d_{accx}x_4 & 0 & 0 \\ 0 & -g \sin x_2 \sin x_5 & Mx_4 & Mx_3 + 2m_{acc}d_{accxy}x_4 & g \cos x_2 \cos x_5 & 0 \\ 0 & 0 & 0 & 0 & -g \sin x_5 & 0 \\ 0 & 0 & 0 & 0 & 0 & 0 \end{pmatrix} \quad (45)$$

(a)  $x_l$  and  $\hat{x}_l$ (b)  $\alpha$  and  $\hat{\alpha}$ (c)  $\dot{x}_l$  and  $\hat{\dot{x}}_l$ (d)  $\dot{\alpha}$  and  $\hat{\dot{\alpha}}$ (e)  $\dot{x}_l$  and  $\hat{\dot{x}}_l$ 

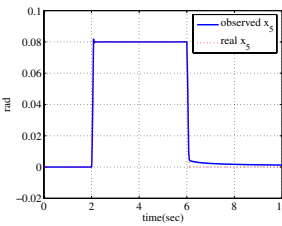
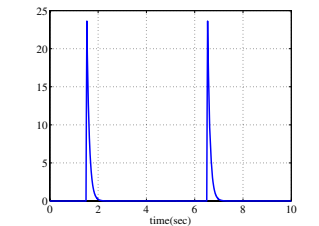
(f) applied torque pattern

(g)  $\dot{x}_l$  and  $\hat{\dot{x}}_l$ 

(h) applied yaw moment

(i)  $\dot{x}_l$  and  $\hat{\dot{x}}_l$ 

(j) applied torque pattern

(k)  $\dot{x}_l$  and  $\hat{\dot{x}}_l$ 

(l) applied yaw moment

Fig. 9. Simulation 2) Climbing with the heading angle  $\frac{\pi}{3}$ Fig. 10. Simulation 3) Attempts to change  $\alpha$ 

In this case, the simulation results show that the proposed observer also estimate the states correctly.

## V. CONCLUSION

In this paper, an extended operational state observer is proposed. It can estimate the heading angle of a wheelchair and the slope angle on which the wheelchair is as well as wheelchair's moving velocity.

Simplified motion equations of a wheelchair in the longitudinal and lateral directions are derived and utilized in the design of the observer. Considering the nonlinear characteristics of these motions, the Extended Kalman Filter design is adopted. Simulation results verify this observer correctly estimates all states in various operational environments.

The verification by simulations only certify the EKF al-

gorithm is right. Motion equations and output equations derived in this paper cannot be verified in the simulations. To see the appropriateness of these equations, experiments using real wheelchairs should be conducted. This is future work.

#### REFERENCES

- [1] Sehoon Oh and Yoichi Hori, "Development of Noise Robust State Observer for Power Assisting Wheelchair and its Applications," *IPEC-Niigata*, pp.1971-1975, 2005.
- [2] T. Söderström, *Discrete-time Stochastic Systems*, 2002.
- [3] Simon J.Julier and Jeffrey K. Uhlmann, "Unscented Filtering and Nonlinear Estimation," *Proceedings of the IEEE*, pp. 401-422, Vol.92, No.3, 2004.